Supplementary Information

Achieving Multi-Stimuli-Responsive and Color-Tunable Luminescence from Ultralong Organic Phosphorescent Materials

Lu Zhou,[ab‡] Yu Yan,[b‡] Jianzhong Fan,[c] Qingfang Mu,[c] Xiangchun Li[b] and Wen-Yong Lai*[b]

[a] Jiangsu Key Laboratory of Industrial Online Detection and Intelligent Perception & Institute of Electrical Engineering, Nanjing Vocational University of Industry Technology, 1 Yangshan Road, Nanjing 210023, China

[b] State Key Laboratory of Flexible Electronics (LoFE), Institute of Advanced Materials (IAM), School of Chemistry and Life Sciences, Nanjing University of Posts & Telecommunications, 9 Wenyuan Road, Nanjing 210023, China.

[c] Shandong Province Key Laboratory of Medical Physics and Image Processing Technology, School of Physics and Electronics, Shandong Normal University, Jinan 250358, China.

‡ L. Z. and Y. Y. are co-first authors with equal contribution to this work.

* E-mail: iamwylai@njupt.edu.cn

I. Experimental section

Measurements

Nuclear magnetic resonance (^{1}H and ^{13}C NMR) spectra were collected using Bruker Avance III Nuclear Magnetic Resonance. Chemical shift was relative to tetramethylsilane (TMS) as the internal standard. Resonance patterns were reported with the notation *s* (singlet), *d* (double), *t* (triplet), *q* (quartet), and *m* (multiplet); UV-visible absorption spectra were obtained using Perkin Elmer Lambda 35; Steady-state fluorescence/phosphorescence spectra and excitation spectra were measured using Hitachi F-4600; The lifetimes and time-resolved emission map were carried out on Edinburgh FLSP 980 fluorescence spectrophotometer equipped with a xenon arc lamp (Xe 900) and microsecond flash-lamp (μF900), respectively; Single crystal X-ray diffraction (SC-XRD) experiments were carried out using a Bruker D8 QUEST X-ray single crystal diffractometer; Powder X-ray diffraction (XRD) patterns were measured using a Bruker D8 Advance diffractometer; Luminescent photos and videos were taken by cell phone with a handheld UV-lamp on and off.

Material synthesis

The starting materials, like phenothiazine, 3-bromo-10H-phenothiazine, iodobenzene, 1-bromo-4-iodobenzene, and bis(pinacolato)diboron, were commercially available, which were used as received. All chemicals were purchased from commercial suppliers and used directly without further purification. The target products were synthesized according to reported methods. All the molecules synthesized were purified by column chromatography and recrystallization from dichloromethane and *n*-hexane for two times, and fully characterized by ^{1}H NMR, ^{13}C NMR and HRMS.

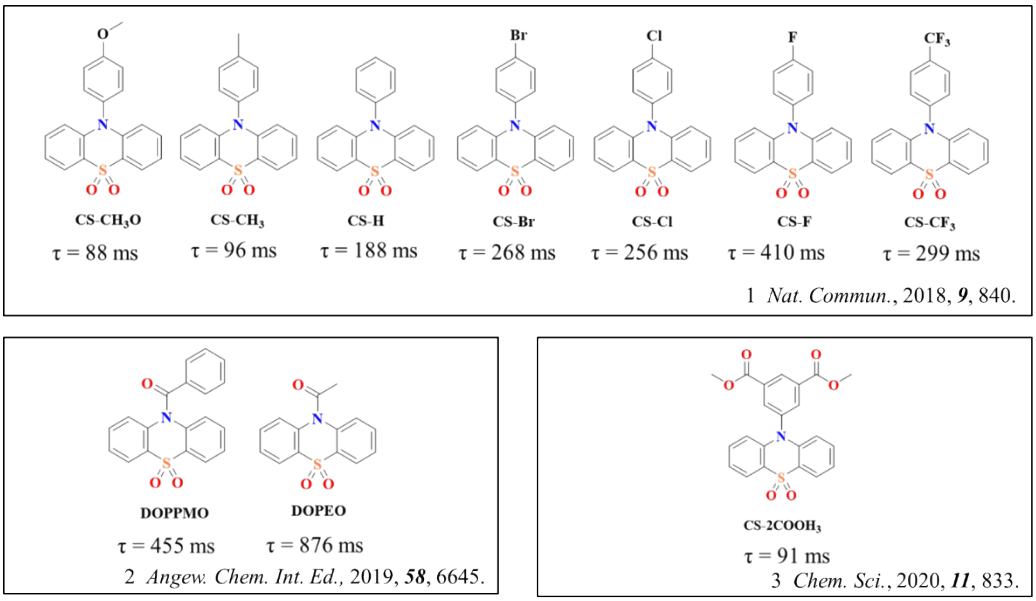

Figure S1. Molecular structures and UOP lifetime of the reported phenothiazine 5,5-dioxide UOP derivatives based on PTZO units.

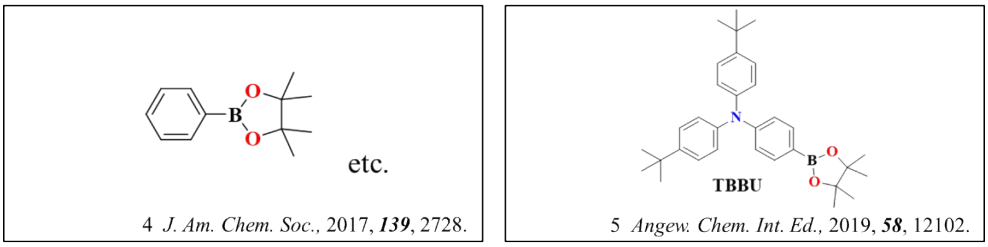

Figure S2. Molecular structures of the reported arylboronic ester UOP derivatives.

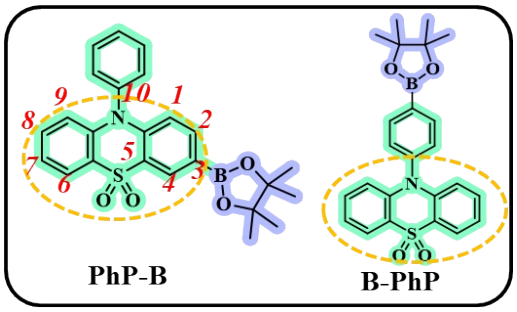

Scheme S1. Molecular structures of PhP-B and B-PhP.

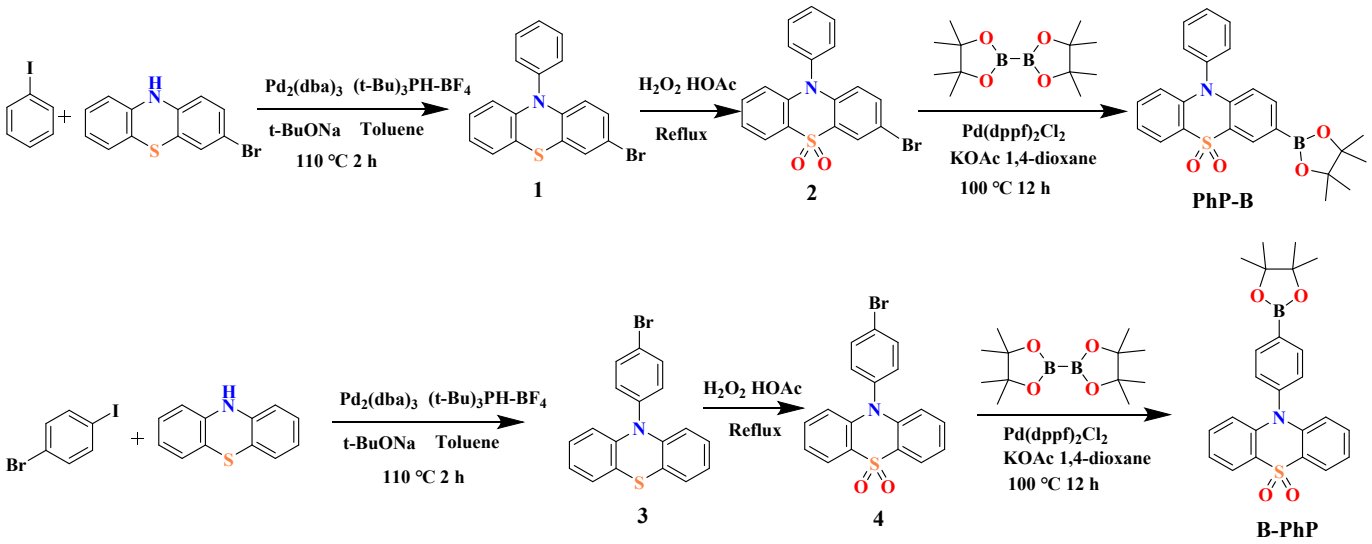

Scheme S2. Synthetic routes of the target compounds PhP-B and B-PhP.

PhP-B:

Step1: 3-bromo-10H-phenothiazine (1.12 g, 4 mmol), iodobenzene (2.45 g, 12 mol), sodium tert-butoxide (0.77 g, 8 mmol) and tri-tert-butylphosphonium tetrafluoroborate (0.12 g, 0.4 mmol) were added into a 100 mL flask. Then the catalyst tris(dibenzylideneacetone)dipalladium (0.18 g, 0.2 mmol) was added under nitrogen atmosphere. The resultant mixture was dissolved in toluene (30 mL) and refluxed for 2 hours under nitrogen, then extracted with dichloromethane and saturated sodium chloride solution. The combined organic extracts were dried over anhydrous Na_2SO_4 and concentrated by rotary evaporation. The crude product was purified by column chromatography on silica gel using petroleum ether and dichloromethane (4:1, V:V) as eluent to afford a white solid (intermediate 1) in a yield of 75%.

Step 2: The intermediate 1 (1.06 g, 3 mmol) was dissolved in acetic acid (20 mL) and H_2O_2 (3 mL). After reacting for another 4 hours at 120℃, the reaction mixture was purified *via* recrystallization to a yellowish solid (intermediate 2) in 90% yield.

Step 3: The intermediate 2 (1.04 g, 2.7 mmol), dried bis(pinacolato)diboron (1.37 g, 5.4 mmol) and dried potassium acetate (0.79 g, 8.1 mmol) were added into a 100 mL flask. Then the catalyst [1, 1'-bis(diphenylphosphino) ferrocene] dichloropalladium (II) (0.37 g, 0.5 mmol) was added in nitrogen and dark conditions. The resultant mixture was dissolved in 1, 4-dioxane (30 mL) and refluxed for 24 hours under nitrogen, then extracted with dichloromethane and saturated sodium chloride solution. The combined organic extracts were dried over anhydrous Na_2SO_4 and concentrated by rotary evaporation. The crude product was purified by column chromatography on silica gel using petroleum ether and ethyl acetate (2:1, V:V) as eluent, and recrystallization from dichloromethane and *n*-hexane for three times to afford a white solid (target product) in a yield of 80%. ^{1}H NMR (400 MHz, $CDCl_3$): δ 8.21-8.12 (m, 4H), 7.51-7.30 (m, 5H), 7.24 (d, 1H), 6.64 (d, J = 8.6 Hz, 2H), 1.43(s, 12H). ^{13}C NMR (100 MHz, $CDCl_3$) δ 142.44, 140.51, 138.85, 138.57, 132.72, 131.36, 130.82, 130.35, 129.79, 123.56, 123.25, 122.30, 122.14, 117.36, 116.25, 84.15, 24.85.

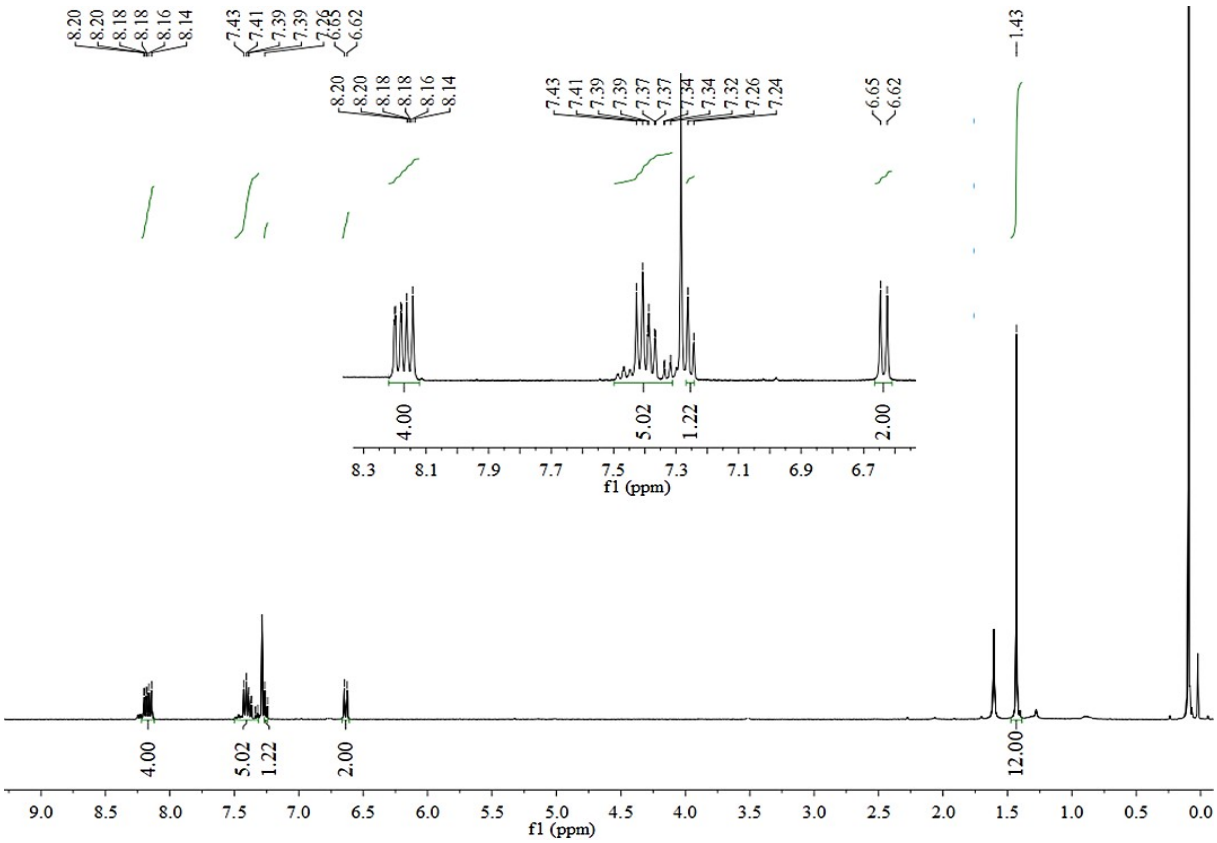

Figure S3. The ^{1}H NMR spectrum of PhP-B in $CDCl_3$ solution.

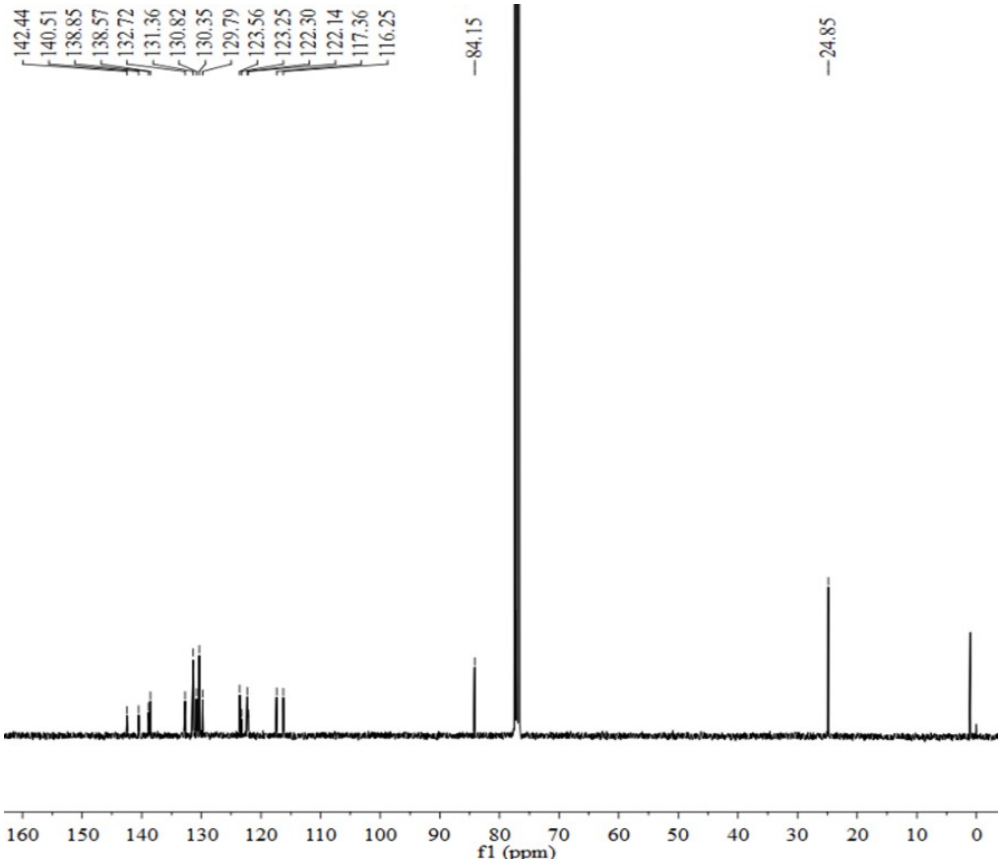

Figure S4. The ^{13}C NMR spectrum of PhP-B in $CDCl_3$ solution.

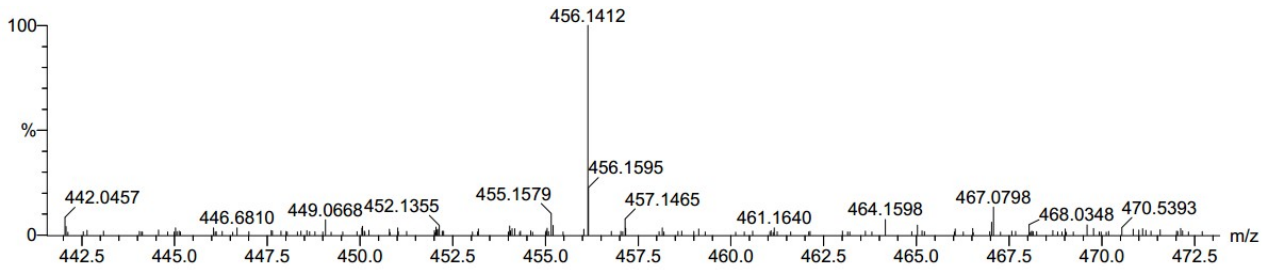

Figure S5. The HRMS spectra of PhP-B.

B-PhP:

Step1: Phenothiazine (1.99 g, 10 mmol), 1-bromo-4-iodobenzene (5.67 g, 20 mol), sodium tert-butoxide (1.92 g, 20 mmol) and tri-tert-butylphosphonium tetrafluoroborate (0.3 g, 1 mmol) were added into a 100 mL flask. Then the catalyst tris(dibenzylideneacetone)dipalladium (0.46 g, 0.5 mmol) was added under nitrogen atmosphere. The resultant mixture was dissolved in toluene (30 mL) and refluxed for 1.5 hours under nitrogen, then extracted with dichloromethane and saturated sodium chloride solution. The combined organic extracts were dried over anhydrous Na_2SO_4 and concentrated by rotary evaporation. The crude product was purified by column chromatography on silica gel using petroleum ether and dichloromethane (4:1, V:V) as eluent to afford a Greenish white solid (intermediate 3) in a yield of 70%.

Step 2: The intermediate 3 (1.06 g, 3 mmol) was dissolved in acetic acid (20 mL) and H_2O_2 (3 mL). After reacting for another 4 hours at 120℃, the reaction mixture was purified *via* recrystallization to a yellowish solid (intermediate 4) in 85% yield.

Step 3: The intermediate 4 (1.04 g, 2.7 mmol), dried bis(pinacolato)diboron (1.37 g, 5.4 mmol) and dried potassium acetate (0.79 g, 8.1 mmol) were added into a 100 mL flask. Then the catalyst [1, 1'-bis(diphenylphosphino) ferrocene] dichloropalladium (II) (0.37 g, 0.5 mmol) was added in nitrogen and dark conditions. The resultant mixture was dissolved in 1,4-dioxane (30 mL) and refluxed for 24

hours under nitrogen, then extracted with dichloromethane and saturated sodium chloride solution. The combined organic extracts were dried over anhydrous Na_2SO_4 and concentrated by rotary evaporation. The crude product was purified by column chromatography on silica gel using petroleum ether and dichloromethane (1:3, V:V) as eluent, and recrystallization from dichloromethane and *n*-hexane for three times to afford a white solid (target product) in a yield of 75%. ^{1}H NMR (400 MHz, DMSO): δ 8.16-8.01 (m, 4H), 7.56 (ddd, J = 16.0, 8.7, 4.9 Hz, 4H), 7.36 (t, J = 7.3 Hz, 4H), 6.63 (d, J = 8.6 Hz, 4H), δ 1.36 (s, 12H). ^{13}C NMR (100 MHz, $CDCl_3$): δ 141.39, 140.60, 137.70, 132.73, 129.79, 123.41, 122.60, 122.05, 117.23, 84.42, 24.94.

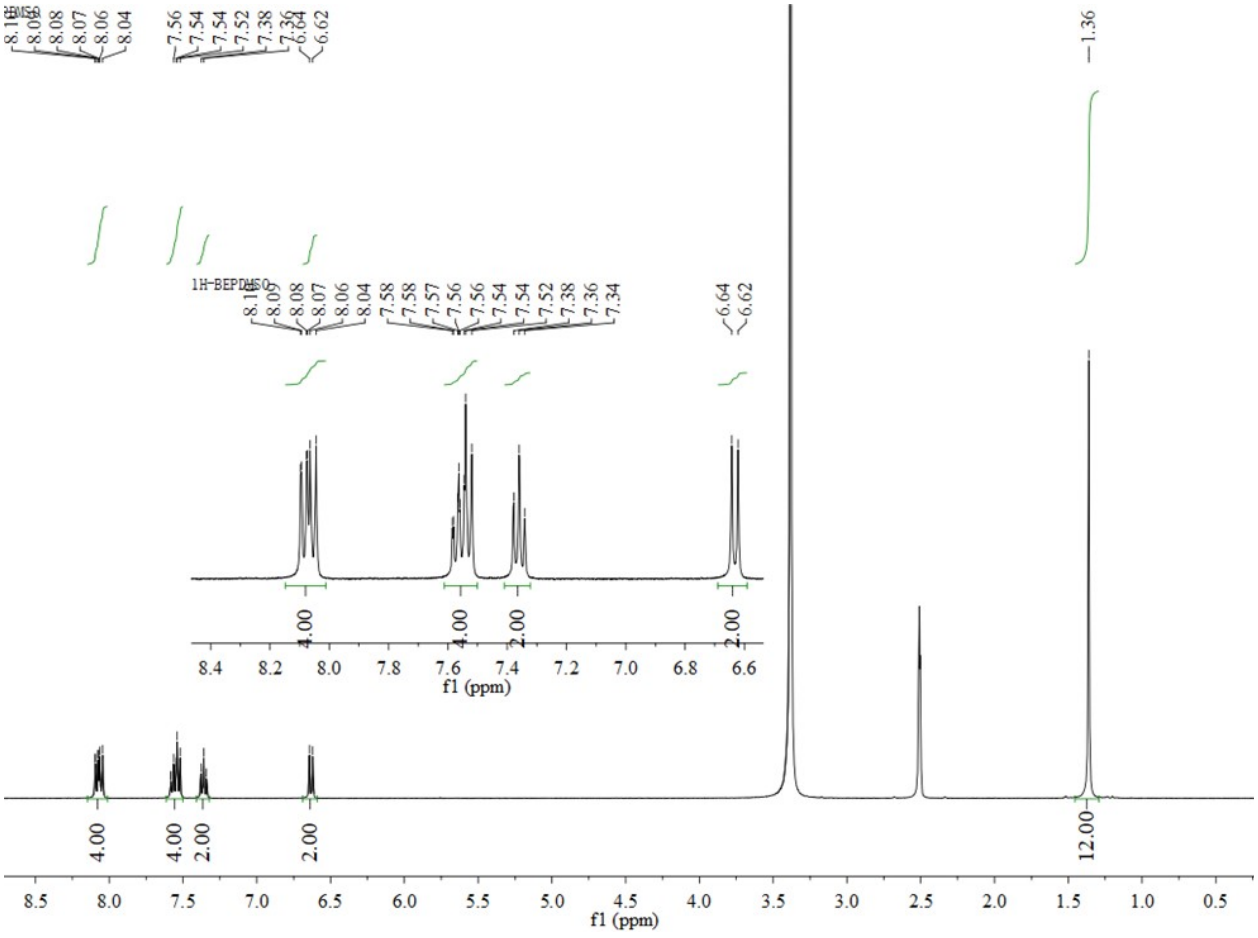

Figure S6. The ^{1}H NMR spectrum of B-PhP in DMSO-d_6 solution.

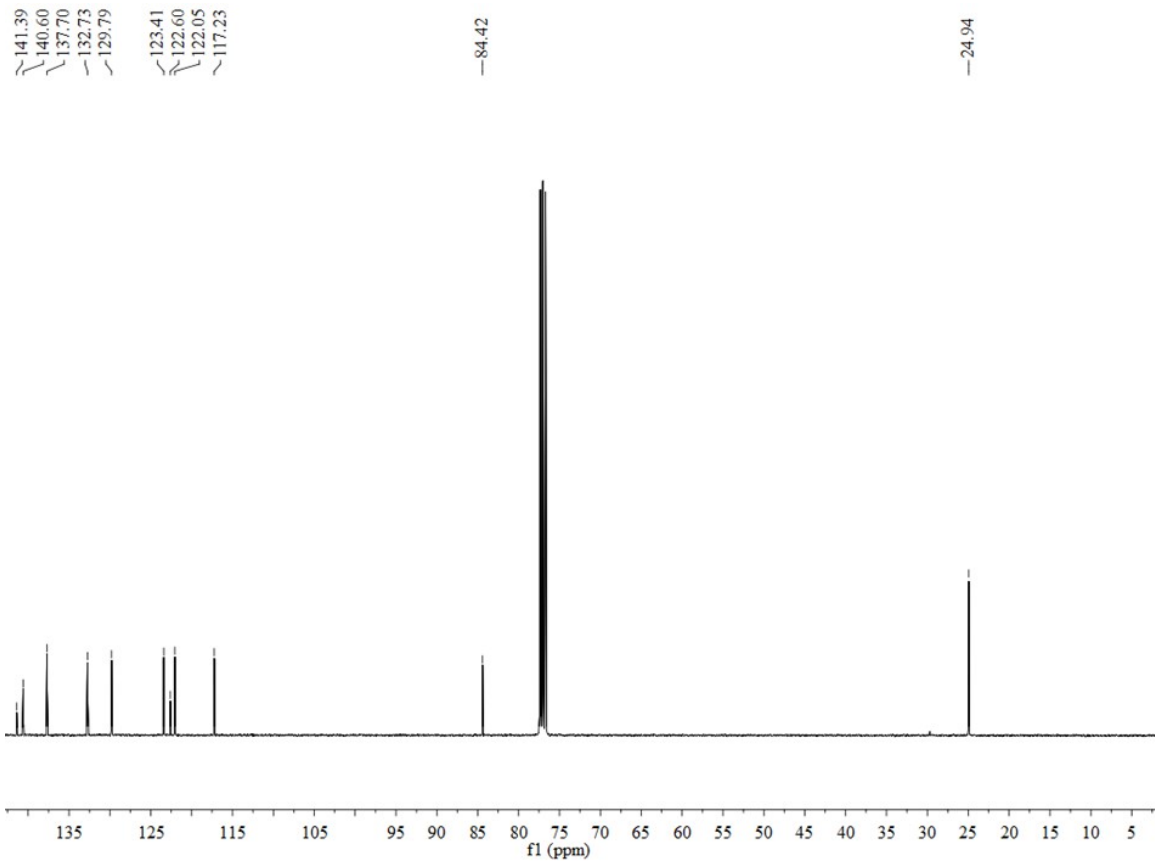

Figure S7. The ^{13}C NMR spectrum of B-PhP in $CDCl_3$ solution.

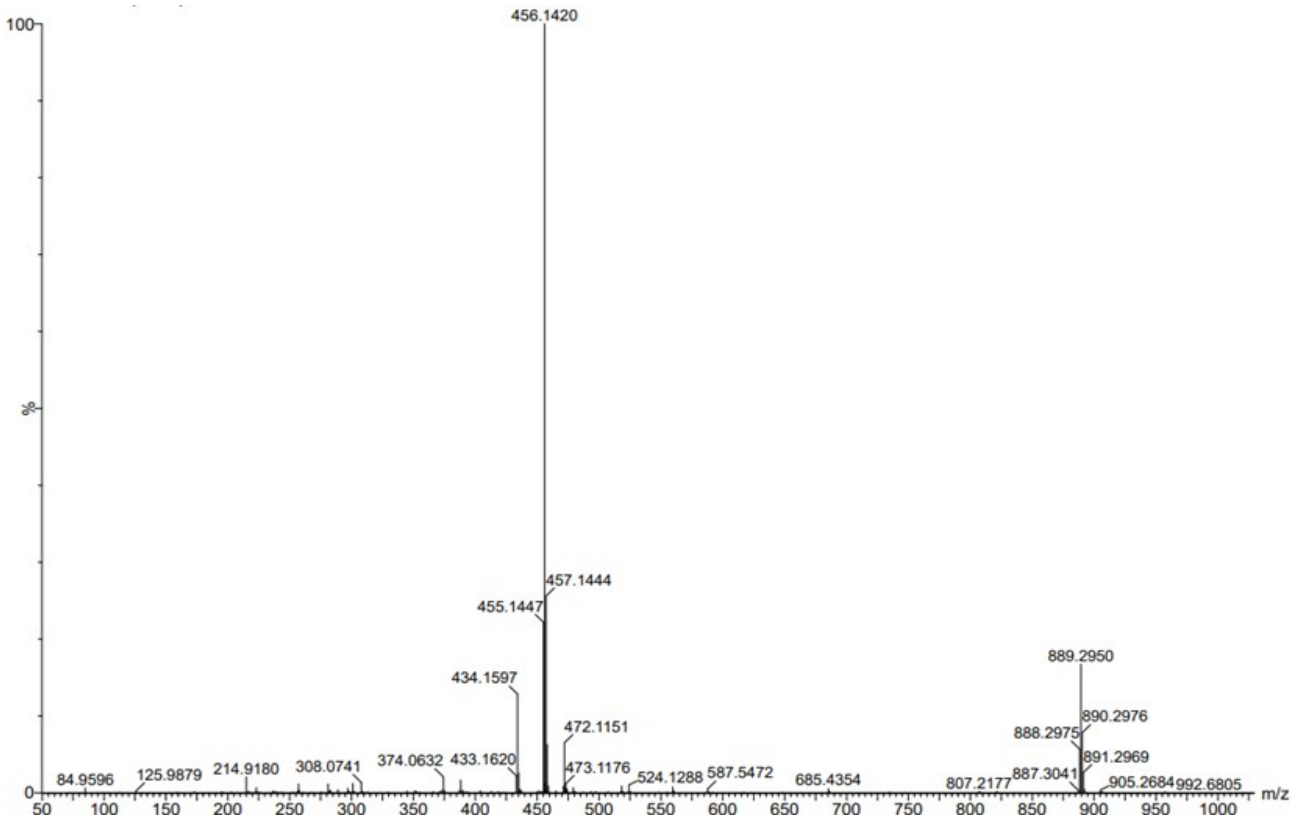

Figure S8. The HRMS spectra of B-PhP.

Crystal cultivation

The crystals of the above compounds were cultivated under similar conditions. The compounds (150 mg) were dissolved in a solvent mixture containing 2 mL tetrahydrofuran and 1 mL *n*-hexane. Then the solutions were kept under ambient conditions to let the solvent be evaporated slowly. Transparent needle-like single crystals of PhP-B were formed in the solution.

II. Additional photophysical properties

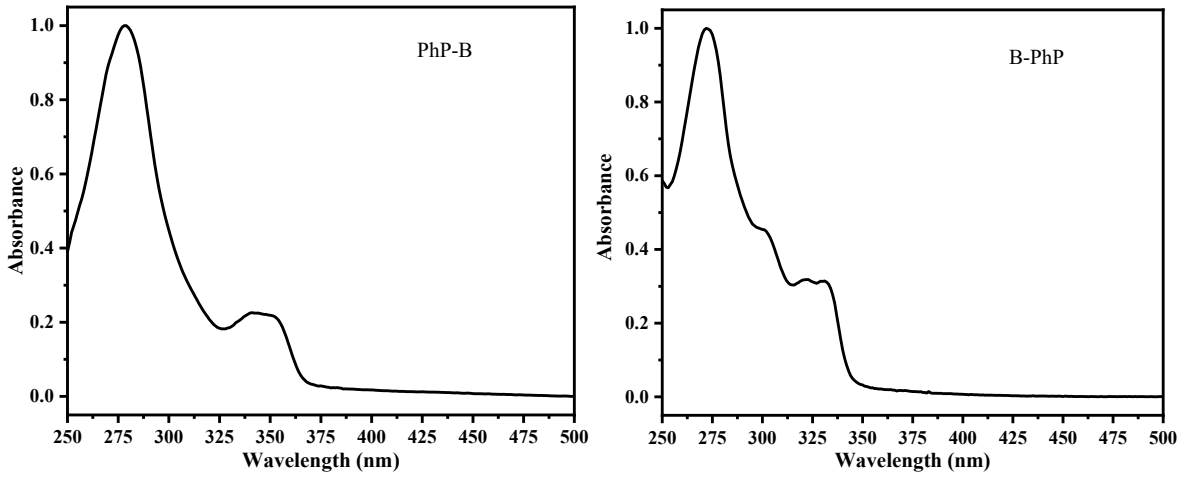

Figure S9. Normalized absorption of PhP-B (left) and B-PhP (right) in dilute THF solution (10^{-5} M) at room temperature under ambient conditions.

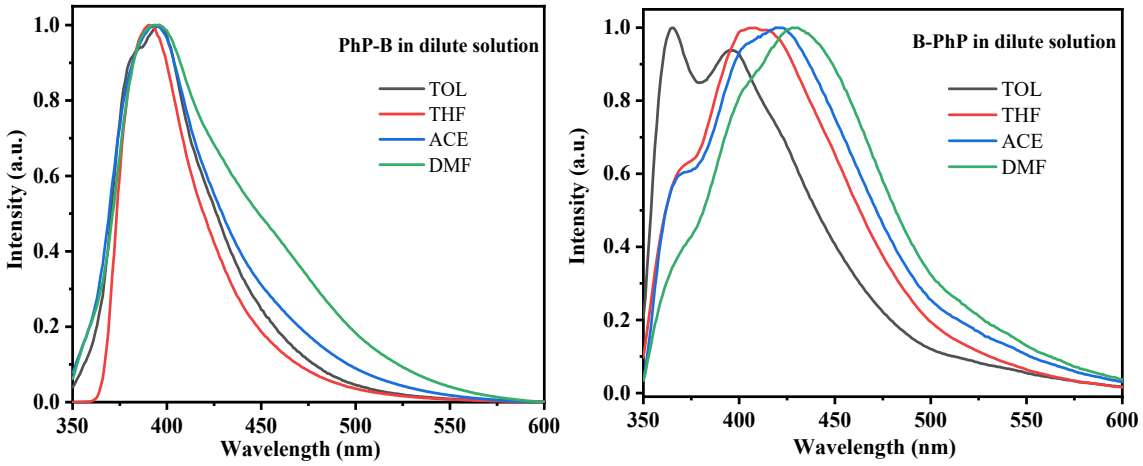

Figure S10. PL spectra of PhP-B (left) and B-PhP (right) in different dilute solutions (10^{-5} M in TOL, THF, ACE and DMF solvents) at room temperature under ambient conditions.

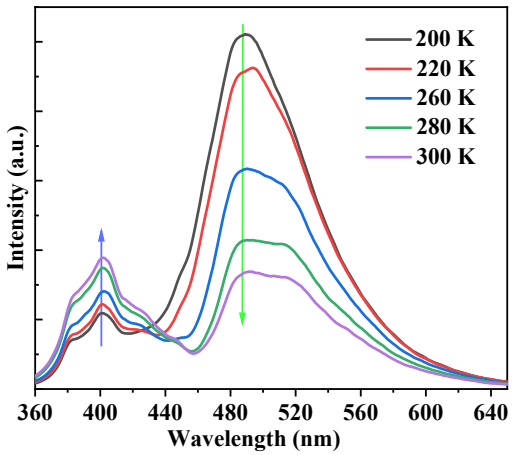

Figure S11. Variable temperature PL spectra of PhP-B crystals from 200 K to 300 K when excited at 340 nm.

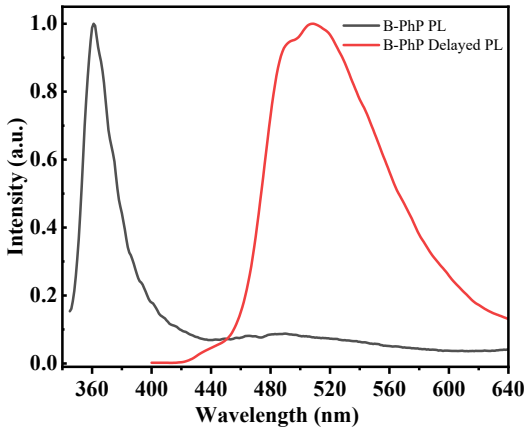

Figure S12. Steady-state PL spectra and delayed PL spectra of B-PhP crystals at room temperature under ambient conditions.

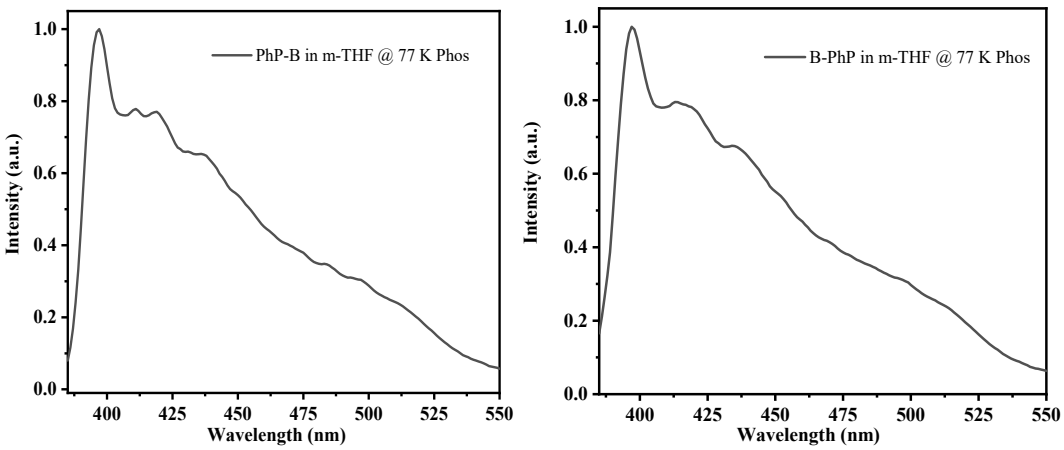

Figure S13. Phosphorescence spectra of PhP-B (left) and B-PhP (right) in 2-methyltetrahydrofuran (5.0×10^{-5} M) at low temperature under ambient conditions.

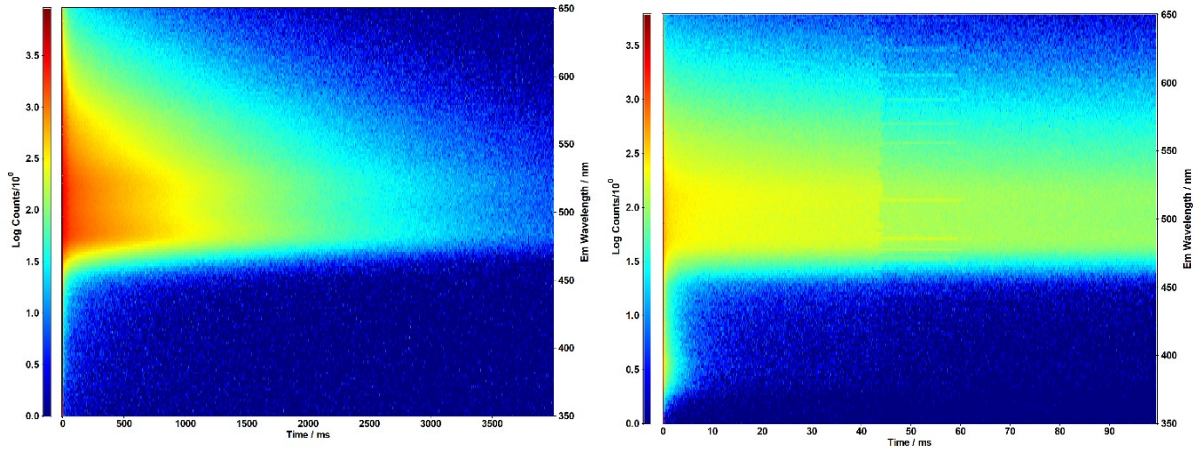

Figure S14. Time-resolved emission maps of PhP-B crystals at room temperature under ambient conditions (left: time range of 4 s; right: time range of 0.1 s).

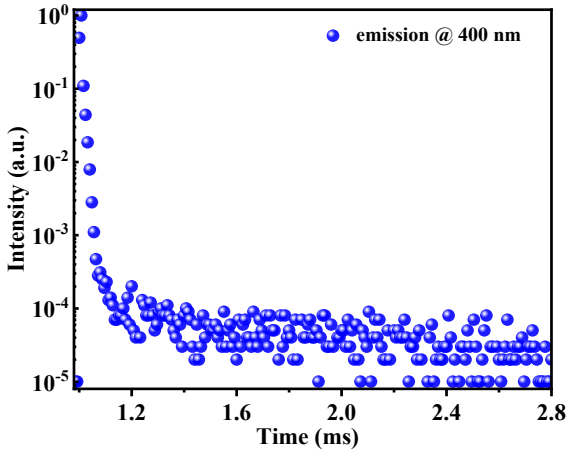

Figure S15. Decay profile of 400 nm emission of PhP-B crystals when excited at 340 nm at room temperature.

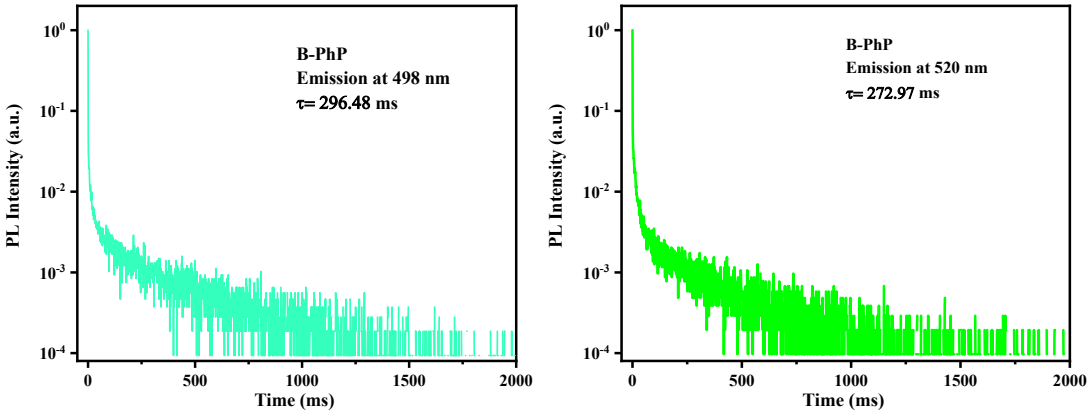

Figure S16. Lifetime decay profiles of the phosphorescence emission bands of B-PhP crystals at room temperature under ambient conditions.

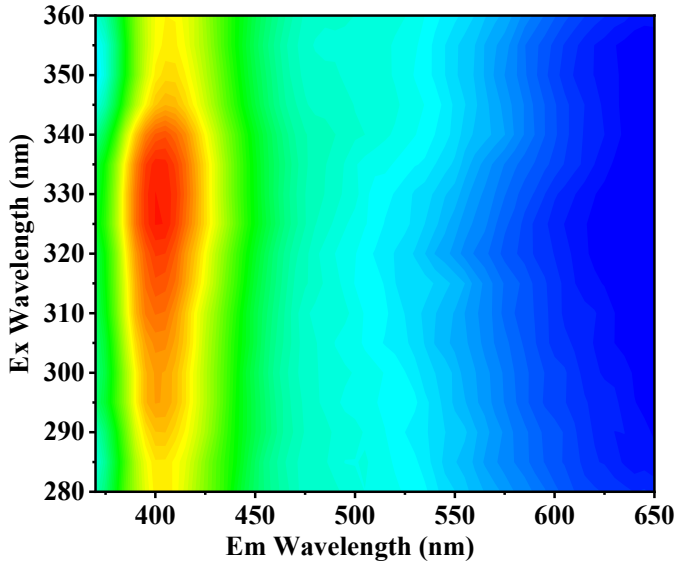

Figure S17. Excitation-emission mapping of steady PL emission of PhP-B crystals at room temperature under ambient conditions.

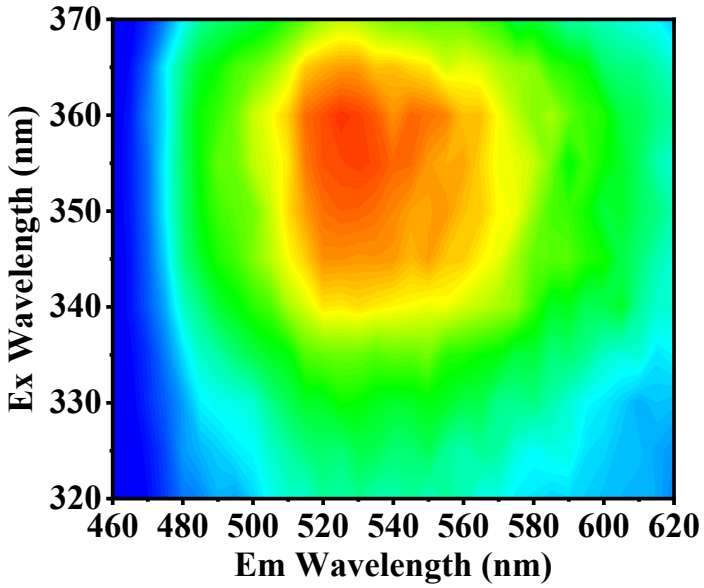

Figure S18. Excitation-emission mapping of UOP emission of PhP-B crystals at room temperature under ambient conditions.

Table S1. Phosphorescence lifetimes (τ) of PhP-B and B-PhP crystals at room temperature under ambient conditions.

Compound	Emission Wavelength (nm)	Phosphorescence						
		τ_1 (ms)	A_1 (%)	τ_2 (ms)	A_2 (%)	τ_3 (ms)	A_3 (%)	τ_{ave} (ms)
PhP-B	490	655.50	86.16	196.53	12.24	28.62	1.60	589.29
	520	657.68	84.18	209.96	13.66	32.83	2.17	583.03
B-PhP	498	296.48	10.67	28.48	20.45	3.79	12.89	37.95
	520	272.97	53.70	23.78	29.22	4.82	17.08	154.36

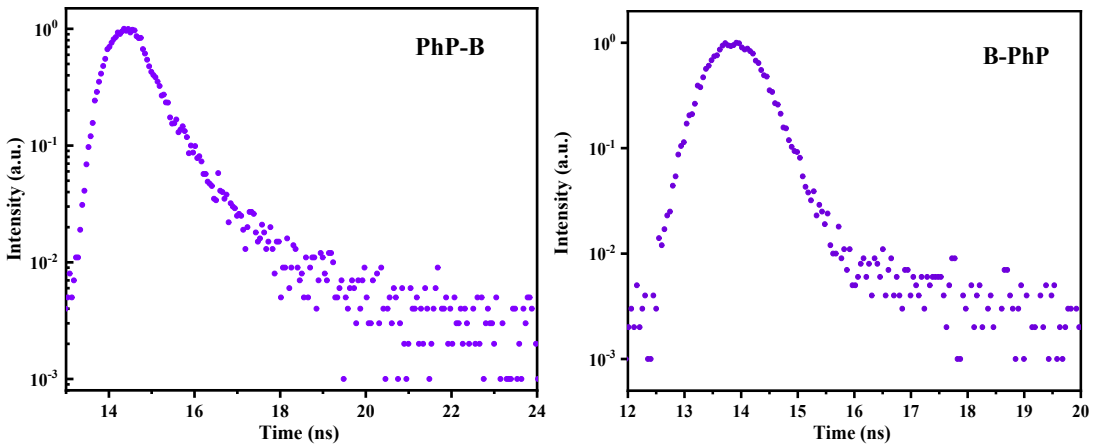

Figure S19. Lifetime decay profiles of the fluorescence emission bands PhP-B (left) and B-PhP (right) crystals at room temperature under ambient conditions.

Table S2. Fluorescence lifetimes (τ) of PhP-B and B-PhP crystals at room temperature under ambient conditions.

Compound	Wavelength (nm)	Fluorescence				
		τ_1 (ns)	A_1 (%)	τ_2 (ns)	A_2 (%)	τ_{ave} (ns)
PhP-B	388	0.55	88.17	1.89	11.83	0.71
B-PhP	360	0.39	98.05	3.62	1.95	0.45

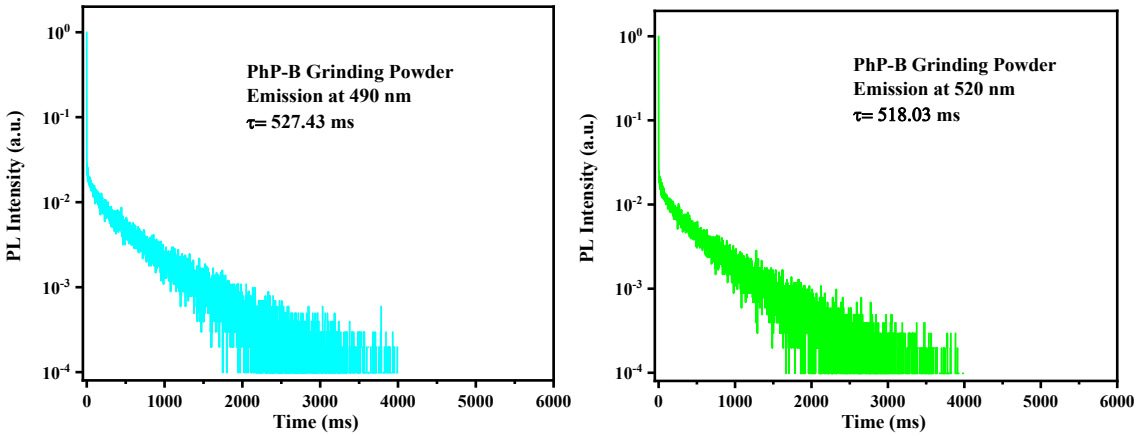

Figure S20. Lifetime decay profiles of the phosphorescence emission bands of PhP-B after grinding at room temperature under ambient conditions.

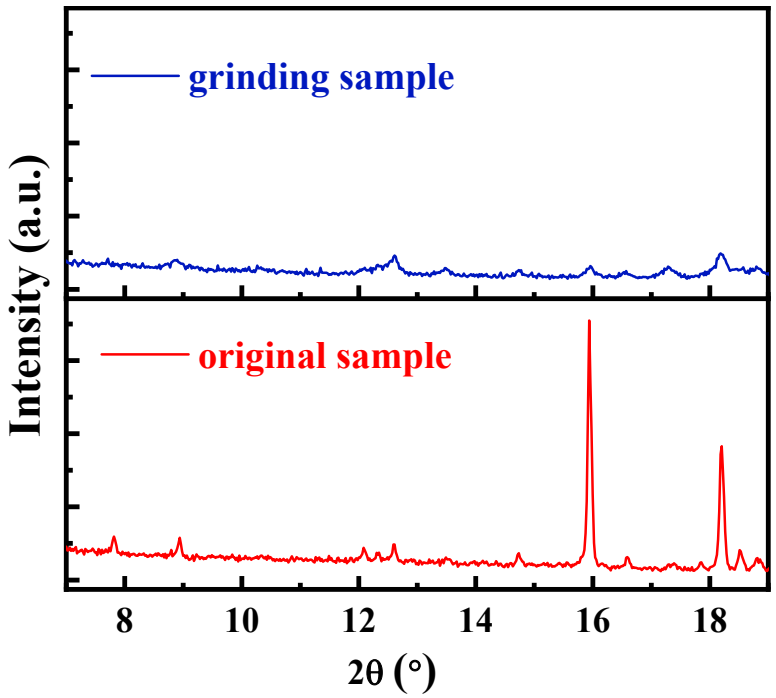

Figure S21. PXRD pattern of PhP-B crystalline powders before/after grinding.

IV. Crystal data and intermolecular interactions

Table S3. Single crystal data for PhP-B

Name		PhP-B
Formula		$C_{24}H_{24}BNO_4S$
Crystal system		triclinic
Space group		P-1
Cell Lengths (Å)	**a**	10.463(12)
	b	10.470(12)
	c	11.199(12)
Cell Angles (°)	**α**	85.87(3)
	β	87.51(3)
	γ	70.20(3)
Cell volume (Å^3)		1151(2)
Z		2
Density (g/cm^3)		1.250
F(000)		456
h_{max}, k_{max}, l_{max}		13, 13, 14
CCDC Number		2045515

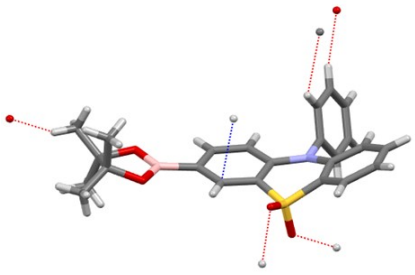

Figure S22. The molecular conformation of PhP-B based on single-crystal structure.

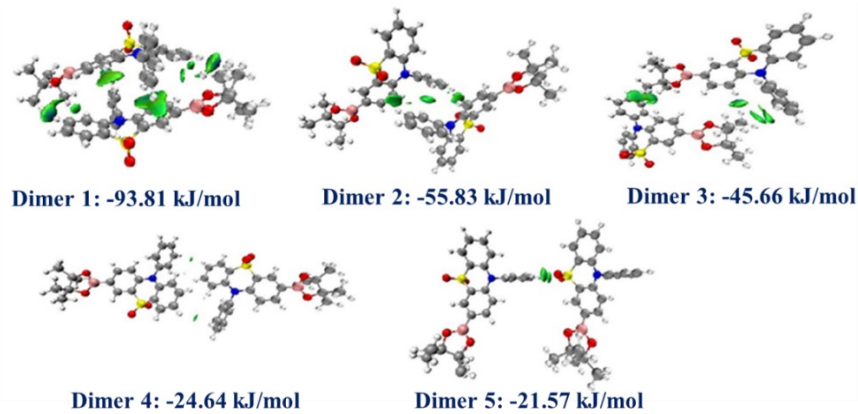

Figure S23. The calculated molecular interactions (green isosurfaces) in different dimers of PhP-B single crystal.

IV. Theoretical calculations

Computational details

Density functional theory (DFT) and time-dependent DFT (TD-DFT) simulations were performed with Gaussian 16 package[1]. All the computational models were built from the single-crystal structures without further geometry optimization. The excitation energy of the n-th singlet state (S_n) and the n-th triplet state (T_n) states were calculated at TD-DFT method of B3LYP/6-31G(d) level based on the monomer and selected dimers extracted from the single-crystal. Frontier molecular orbital distributions were calculated based on the monomer and selected dimers extracted from the single-crystal at B3LYP/6-31G(d).

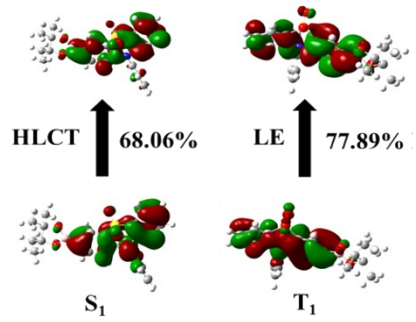

Figure S24. The NTOs of S_1 and T_1 states for monomer. These data are obtained by the time-dependent density functional method at the B3LYP/6-31G*.

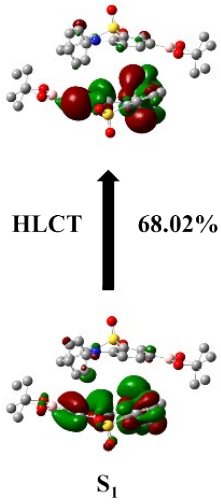

Figure S25. The NTOs of S_1 states for dimer 1. These data are obtained by the time-dependent density functional method at the B3LYP/6-31G*.

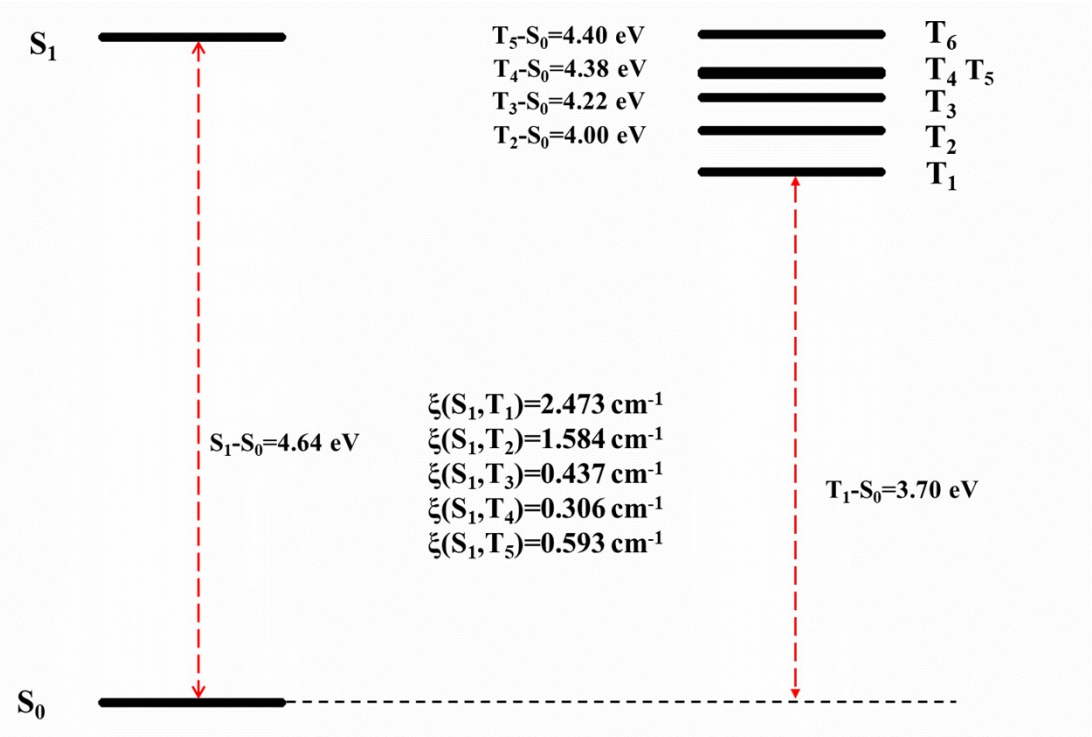

Figure S26. The calculated energy levels based on the PhP-B monomer.

V. Supplementary pictures and videos

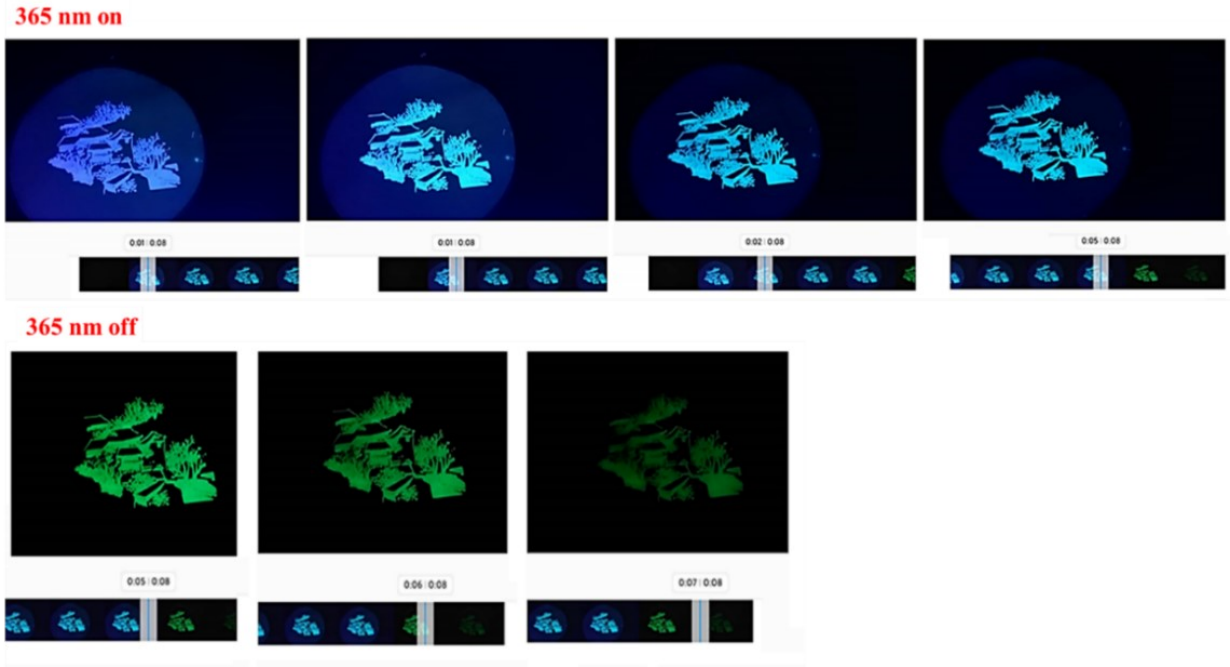

Figure S27. Dynamic emissive patterns prepared by PhP-B crystalline powders *via* screen printing. The complementary pictures and videos were recorded by cell phone MI 9 in dark under ambient conditions

References

[1] Frisch, M. J.; Trucks, G. W.; Schlegel, H. B.; Scuseria, G. E.; Robb, M. A.; Cheeseman, J. R.; Scalmani, G.; Barone, V.; Petersson, G. A.; Nakatsuji, H.; Li, X.; Caricato, M.; Marenich, A. V.; Bloino, J.; Janesko, B. G.; Gomperts, R.; Mennucci, B.; Hratchian, H. P.; Ortiz, J. V.; Izmaylov, A. F.; Sonnenberg, J. L.; Williams-Young, D.; Ding, F.; Lipparini, F.; Egidi, F.; Goings, J.; Peng, B.; Petrone, A.; Henderson, T.; Ranasinghe, D.; Zakrzewski, V. G.; Gao, J.; Rega, N.; Zheng, G.; Liang,W.; Hada, M.; Ehara, M.; Toyota, K.; Fukuda, R.; Hasegawa, J.; Ishida, M.; Nakajima, T.; Honda, Y.; Kitao, O.; Nakai, H.; Vreven, T.; Throssell, K.; Montgomery, J. A., Jr.; Peralta, J. E.; Ogliaro, F.; Bearpark, M. J.; Heyd, J. J.; Brothers, E. N.; Kudin, K. N.; Staroverov, V. N.; Keith, T. A.; Kobayashi, R.; Normand, J.; Raghavachari, K.; Rendell, A. P.; Burant, J. C.; Iyengar, S. S.; Tomasi, J.; Cossi, M.; Millam, J. M.; Klene, M.; Adamo, C.; Cammi, R.; Ochterski, J. W.; Martin, R. L.; Morokuma, K.; Farkas, O.; Foresman, J. B.; Fox, D. J., Gaussian 16 Rev. A.03. 2016.